$\times 10^4$ m/s, and group velocity = 8.4×10^3 m/s at frequency = 3.5 GHz for the case of $d = 20$ μm, $a = 10$ μm, and $w = 100$ μm. The potential in this case decays below 10 percent of its peak when it is away from the wall by 0.2 wavelength. This represents the extent of the energy concentration and at the same time the extent of nonreciprocity of the waveguide. The knowledge about the mode treated here immediately gives us an idea that the proposed structure is effectively available for isolators, circulators, and so forth in a way similar to the edge-guided mode in a ferrite loaded stripline [8].

As mentioned in Section I, the authors would like to have made clear not only that the proposed waveguide is promising in the field of MSW devices, but also that the BEM is useful for the analysis of structures for which analytical solutions are not obtained simply or easily. It may be worthwhile to point out that the computer program developed by the authors makes complex computations possible in such cases as a disc and periodically corrugated waveguides.

References

[1] K. Yashiro, M. Miyazaki, and S Ohkawa, "Boundary element method approach to magnetostatic wave problems," *IEEE Trans. Microwave Theory Tech.*, vol. MTT-33, pp. 248–253, Mar. 1985.

[2] C. A. Brebbia, *The Boundary Element Method for Engineers*. London: Pentech Press, 1978.

[3] H. Tanaka and H. Shimizu, "On the waveguide for magnetostatic surface waves," *Trans. IECE Japan*, vol. J63-B, pp 651–653, June 1980.

[4] F. R. Morgenthaler, "Bound magnetostatic waves controlled by field gradients in YIG single crystals and epitaxial films," *IEEE Trans Magn.*, vol. MAG-14, pp. 806–810, Sept. 1978.

[5] M. Tsutsumi, Y. Masaoka, T. Ohira, and N. Kumagai, "A new technique for magnetostatic wave delay lines," *IEEE Trans. Microwave Theory Tech.*, vol. MTT-29, pp. 583–589, June 1981

[6] K. Yahiro and S. Ohkawa, "Guided magnetostatic waves of the YIG plate magnetized nonuniformly," *IEEE Trans. Microwave Theory Tech.*, vol. MTT-29, pp. 745–747, July 1981.

[7] T. W. O'Keeffe and R. W. Patterson, "Magnetostatic surface-wave propagation in finite samples," *J. Appl. Phys.*, vol. 49, pp. 4886–4895, Sept. 1978

[8] K. Araki, T. Koyama, and Y. Naito, "Reflection problems in a ferrite stripline," *IEEE Trans Microwave Theory Tech.*, vol. MTT-24, pp. 491–498, Aug. 1976.

A New Recurrence Method for Determining the Green's Function of Planar Structures with Arbitrary Anisotropic Layers

RICARDO MARQUÉS, MANUEL HORNO, MEMBER IEEE, AND FRANCISCO MEDINA

Abstract —**A method to determine the Green's functions in the spectral domain is developed. It is suitable for solving the matrix Green's function numerically for an arbitrary anisotropic N-layered dielectric structure. The method is suitable for computation of the characteristic parameters of MIC lines having anisotropic multilayered substrates or superstrates. As an application, the phase velocities of single and coupled microstrips, with a constant gradient of anisotropy along the normal to the interfaces, have been calculated.**

Manuscript received March 12, 1984; revised January 4, 1985.

The authors are with the Departamento de Electricidad y Electrónica, Facultad de Física, Universidad de Sevilla, Seville, Spain.

I. Introduction

During the last several years, the conventional planar structures embedded in anisotropic dielectrics—single [1]–[4], coupled [5]–[8], covered [9]–[11], shielded microstripline [12], [13], slotline [14], and coplanar waveguide [15]—have been analyzed extensively.

The most commonly used anisotropic substrates, such as sapphire and boron–nitride, or some glass- and ceramic-filled polymeric materials, e.g. Duroid and Epsilam, have well-known advantages over the isotropic substrates used largely in microwave integrated circuits. The introduction of anisotropic substrates having tilted principal axes has recently made it possible to manipulate some characteristic parameters of the structure in a range depending on the substrate anisotropy. For instance, it has been shown that the phase velocities can be equalized by varying the tilting angle in the coupled microstriplines [7].

The propagation characteristics study of such structures has been made using various procedures. Nevertheless, the methods utilizing the Green's potential function are used extensively. For instance, if the Green's function in the Fourier domain is known, the unknown quantity becomes the charge density and the problem of estimating the characteristic parameters is easily solved by using the moment approach [5] or variational techniques [4].

The Green's function is generally calculated for each structure. In this paper, a recurrence algorithm is presented to evaluate the transform of the Green's function for planar open structures having multilayered substrates or superstrates with arbitrary anisotropy. The method is useful, for instance, in calculating the capacitance of planar structures with single or coupled strips in one or more interfaces embedded in multilayered anisotropic dielectrics, including an arbitrary gradient of anisotropy in the normal direction to the interfaces, requiring very little modifications in the programs already existing.

II. Recurrence Formulas for the Potential and Fields in an Anisotropic Layer

Let us first consider a layer of perfect and homogeneous dielectric of finite thickness h. The permittivity tensor at the $x-y$ plane is given by

$$\bar{\bar{\epsilon}} = \begin{pmatrix} \epsilon^{11} & \epsilon^{12} \\ \epsilon^{12} & \epsilon^{22} \end{pmatrix}. \quad (1)$$

Then the bidimensional equation for the electrostatic potential in the Fourier domain has the form

$$\epsilon^{22}\frac{\partial^2\tilde{\phi}}{\partial y^2} + 2j\epsilon^{12}\beta\frac{\partial\tilde{\phi}}{\partial y} - \epsilon^{11}\beta^2\tilde{\phi} = 0. \quad (2)$$

The general solution of this differential equation is

$$\tilde{\phi}(\beta, y) = e^{-j\beta R y}(A\sinh(\beta S y) + B\cosh(\beta S y)) \quad (3)$$

where

$$R = \frac{\epsilon^{12}}{\epsilon^{22}} \quad (4)$$

$$S = \left\{\frac{\epsilon^{11}}{\epsilon^{22}} - \left(\frac{\epsilon^{12}}{\epsilon^{22}}\right)^2\right\}^{1/2}. \quad (5)$$

$\tilde{\phi}(\beta, y)$ is the potential Fourier transform y-coordinate and A and B are arbitrary coefficients which must be determined from the boundary conditions.

This way, the y-component of the electrical displacement vector in the Fourier domain can be expressed

$$\tilde{D}_y(\beta, y) = -\beta\epsilon^{eq}\exp(-j\beta R y)(A\cosh(\beta S y) + B\sinh(\beta S y)) \tag{6}$$

where

$$\epsilon^{eq} = S\epsilon^{22}. \tag{7}$$

If the new variable is defined

$$y^{eq} = Sy \tag{8}$$

a relation between $\tilde{\phi}$ and $\tilde{D}_y$ can be expressed as follows:

$$\tilde{\phi}(\beta, y + \Delta y) = e^{-j\beta R\Delta y}\left\{\cosh(\beta\Delta y^{eq})\tilde{\phi}(\beta, y) - \left(\frac{1}{\beta\epsilon^{eq}}\right)\sinh(\beta\Delta y^{eq})\tilde{D}_y(\beta, y)\right\} \tag{9}$$

$$\tilde{D}_y(\beta, y + \Delta y) = e^{-j\beta R\Delta y}\{\cosh(\beta\Delta y^{eq})\tilde{D}_y(\beta, y) - \beta\epsilon^{eq}\sinh(\beta\Delta y^{eq})\tilde{\phi}(\beta, y)\}. \tag{10}$$

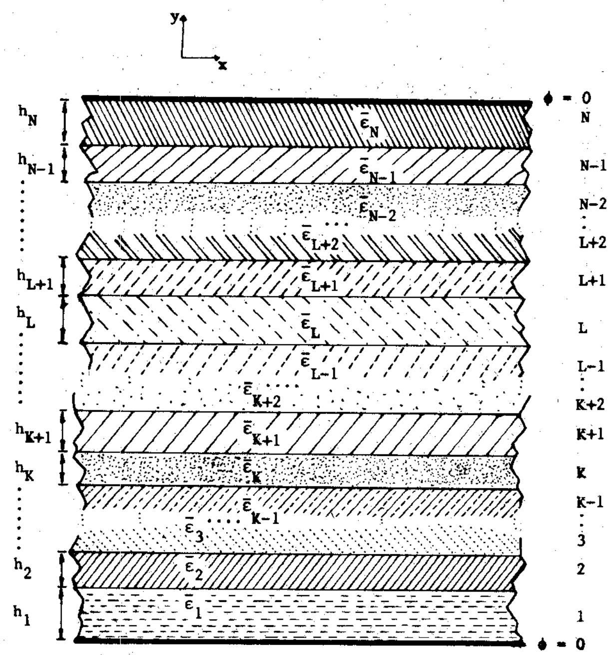

Fig. 1. General N-layered anisotropic structure.

III. Construction of the Green's Function at the Interfaces

Let us consider a more general structure now (Fig. 1). It is composed of N layers of anisotropic substrates having arbitrary tilted principal axes of finite thickness h_n. The upper and lower bounds of the structure are perfect conducting plates. One or more of those layers can be made of isotropic dielectrics or air, and the upper or the lower conducting plates can be shifted to infinity.

If there is no charge density at the interfaces, the recurrence formulas (9) and (10) and the boundary conditions are used to find the following expressions:

$$\tilde{\phi}_0(\beta) = 0 \tag{11a}$$

$$\tilde{D}_{y,0}(\beta) = A \tag{11b}$$

$$\tilde{\phi}_L(\beta) = \exp\left(-j\beta\sum_{n=1}^{L} R_n h_n\right) F_1^L(\beta) A \tag{11c}$$

$$\tilde{D}_{y,L}(\beta) = \exp\left(-j\beta\sum_{n=1}^{L} R_n h_n\right) F_3^L(\beta) A \tag{11d}$$

where $\tilde{\phi}_L(\beta)$ and $\tilde{D}_{y,L}(\beta)$ are the potential and the y-component of the electric displacement vector at the Lth interface.

Similarly it is found that

$$\tilde{\phi}_N(\beta) = 0 \tag{12a}$$

$$\tilde{D}_{y,N}(\beta) = C \tag{12b}$$

$$\tilde{\phi}_{N-K}(\beta) = \exp\left(j\beta\sum_{n=0}^{K-1} R_{N-n} h_{N-n}\right) F_2^K(\beta) C \tag{12c}$$

$$\tilde{D}_{y,N-K}(\beta) = \exp\left(j\beta\sum_{n=0}^{K-1} R_{N-n} h_{N-n}\right) F_4^K(\beta) C \tag{12d}$$

where F_i^j functions can be determined using the recurrence algorithm

$$h_n^{eq} = S_n h_n \tag{13}$$

$$\epsilon_n^{eq} = S_n\epsilon_n^{22} \tag{14}$$

$$R_n = \frac{\epsilon_n^{12}}{\epsilon_n^{22}} \tag{15}$$

$$S_n = \left(\frac{\epsilon_n^{11}}{\epsilon_n^{22}} - R_n^2\right)^{1/2} \tag{16}$$

$$F_1^1 = -\sinh(\beta h_1^{eq})/(\beta\epsilon_1^{eq}) \tag{17a}$$

$$F_2^1 = \sinh(\beta h_N^{eq})/(\beta\epsilon_N^{eq}) \tag{17b}$$

$$F_3^1 = \cosh(\beta h_1^{eq}) \tag{17c}$$

$$F_4^1 = \cosh(\beta h_N^{eq}) \tag{17d}$$

$$F_1^{i+1} = \cosh(\beta h_{i+1}^{eq}) F_1^i - \frac{1}{\beta\epsilon_{i+1}^{eq}}\sinh(\beta h_{i+1}^{eq}) F_3^i \tag{17e}$$

$$F_2^{i+1} = \cosh(\beta h_{N-i}^{eq}) F_2^i + \frac{1}{\beta e_{N-i}^{eq}}\sinh(\beta h_{N-i}^{eq}) F_4^i \tag{17f}$$

$$F_3^{i+1} = \cosh(\beta h_{i+1}^{eq}) F_3^i - \beta\epsilon_{i+1}^{eq}\sinh(\beta h_{i+1}^{eq}) F_1^i \tag{17g}$$

$$F_4^{i+1} = \cosh(\beta h_{N-i}^{eq}) F_4^i + \beta\epsilon_{N-i}^{eq}\sinh(\beta h_{N-i}^{eq}) F_2^i. \tag{17h}$$

Expressions (11), (12), and (17) permit one to calculate the potential and electric displacement vector across any interface, when A and C are specified.

Let us consider a free-charge density sheet at the Lth interface $\rho_L(x)$. The boundary conditions at this interface are

$$\tilde{\phi}\left(\beta, \sum_{n=1}^{L} h_n - 0\right) = \tilde{\phi}\left(\beta, \sum_{n=1}^{L} h_n + 0\right) \tag{18}$$

$$\tilde{D}_y\left(\beta, \sum_{n=1}^{L} h_n - 0\right) + \tilde{\rho}_L(\beta) = \tilde{D}_y\left(\beta, \sum_{n=1}^{L} h_n + 0\right) \tag{19}$$

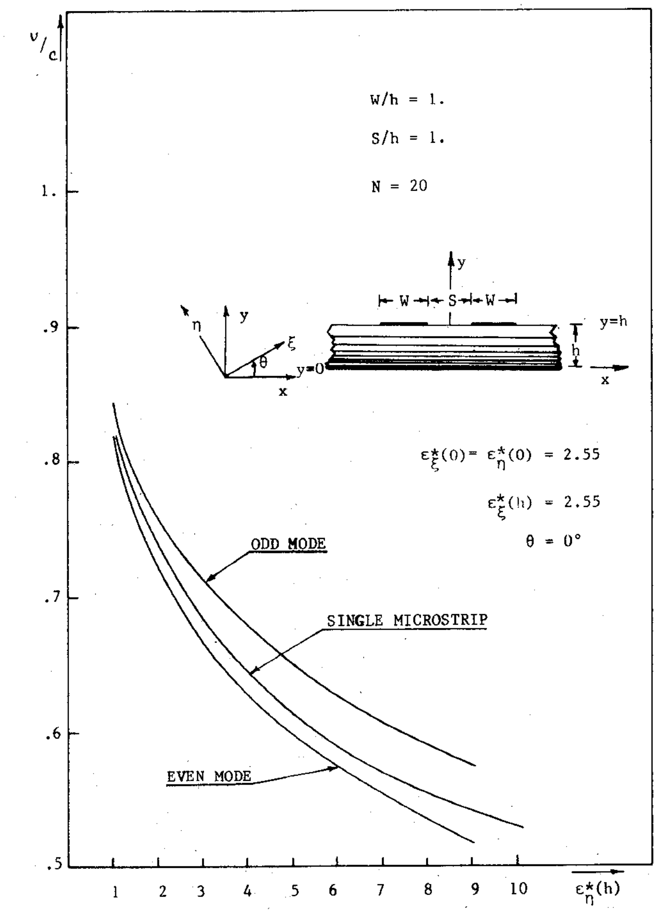

Fig. 2. Variation of normalized phase velocities of coupled microstriplines with a linear variation in the y-direction of ϵ_η^*.

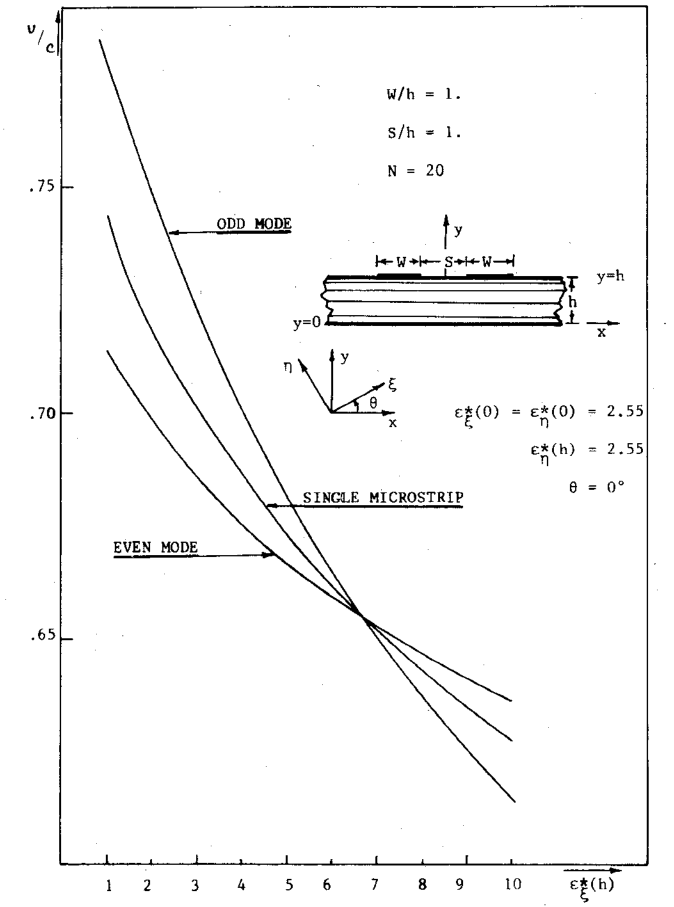

Fig. 3. Variation of normalized phase velocities of coupled microstriplines with a linear variation in the y-direction of ϵ_ξ^*.

where $\tilde{\rho}_L(\beta)$ is the Fourier transform of $\rho_L(x)$. Using the relations (11) and (12), the recurrence formulas (17), and the boundary conditions (18) and (19), the coefficients A and C in (11) and (12) can be determined

$$A = \tilde{\rho}_L(\beta)\exp\left(j\beta\sum_{n=1}^{L} R_n h_n\right)\left\{\frac{F_1^L F_4^{N-L}}{F_2^{N-L}} - F_3^L\right\}^{-1} \tag{20}$$

$$C = \tilde{\rho}_L(\beta)\exp\left(-j\beta\sum_{n=L+1}^{N} R_n h_n\right)\left\{F_4^{N-L} - \frac{F_3^L F_2^{N-L}}{F_1^L}\right\}^{-1}. \tag{21}$$

After calculating A and C, the Green's function $\tilde{G}_{KL}$, which relates the potential $\tilde{\phi}_K(\beta)$ at the Kth interface with the source charge density $\tilde{\rho}_L(\beta)$ at the Lth interface

$$\tilde{\phi}_K(\beta) = \tilde{G}_{KL}(\beta)\tilde{\rho}_L(\beta) \tag{22}$$

can be easily calculated

$$\tilde{G}_{KL} = \exp\left(j\beta\sum_{i=K+1}^{L} R_i h_i\right)\left\{\frac{F_1^L F_4^{N-L}}{F_1^K F_2^{N-L}} - \frac{F_3^L}{F_1^K}\right\}^{-1} \tag{23a}$$

for $K < L$

$$\tilde{G}_{KK} = \left\{\frac{F_4^{N-K}}{F_2^{N-K}} - \frac{F_3^K}{F_1^K}\right\}^{-1} \tag{23b}$$

and, using the reciprocity Green's theorem for electrostatics [16], which can be easily extended to anisotropic lossless media, and after expressing it in the Fourier domain through the Parseval's theorem

$$\tilde{G}_{KL}(\beta) = G_{LK}^*(\beta) \tag{23c}$$

where the superscript * indicates the complex conjugate; that is, the $[\tilde{G}_{KL}]$ matrix is a Hermitian matrix.

When β increases ($\beta \to \infty$), the expressions (23a) and (23b) become inadequate for computation. In order to avoid that, rescaled expressions can be used for high values of β (see Appendix).

The recurrence character of relations (23) makes them suitable for direct computation. Without further modifications, we can use the already existing programs to calculate the characteristics of multilayered related structures, introducing those relations in these programs, where the number of layers can be treated as an input in the programs.

IV. Application

As a numeric application of this technique, the normalized phase velocities of coupled microstrips on an anisotropic substrate with a y-directed gradient of its permittivity tensor have been calculated (Figs. 2–4). This tensor is assumed to be, in the

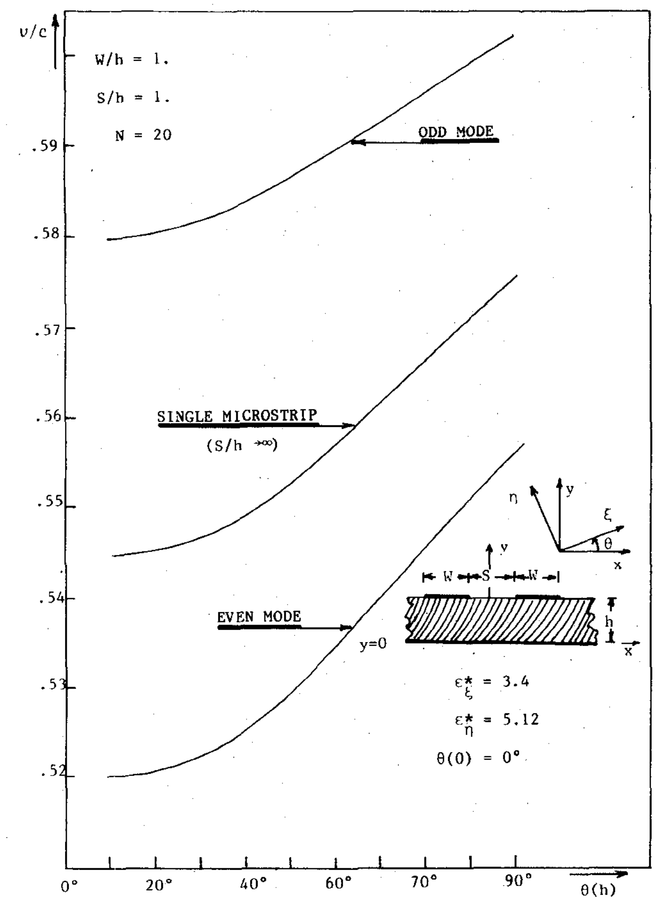

Fig. 4. Variation of normalized phase velocities of coupled microstriplines with a linear variation in the y-direction of θ.

$x-y$ plane

$$\bar{\bar{\epsilon}} = \begin{pmatrix} \epsilon^{11} & \epsilon^{12} \\ \epsilon^{12} & \epsilon^{22} \end{pmatrix}$$

$$\epsilon^{11} = \epsilon_0\left(\epsilon_\xi^*(y)\cos^2\theta(y) + \epsilon_\eta^*(y)\sin^2\theta(y)\right)$$

$$\epsilon^{12} = \epsilon_0\left(\epsilon_\xi^*(y) - \epsilon_\eta^*(y)\right)\sin\theta(y)\cos\theta(y)$$

$$\epsilon^{22} = \epsilon_0\left(\epsilon_\xi^*(y)\sin^2\theta(y) + \epsilon_\eta^*(y)\cos^2\theta(y)\right) \tag{24}$$

where ϵ_ξ^* and ϵ_η^* denote the values of the relative permittivity along the principal axes of the dielectric, and θ the angle of tilting between the ξ- and x-axes.

To achieve this, we have subdivided the substrate thickness into N homogeneous layers of constant permittivities, equal to those of their middle points. Then, applying the trial function for the charge density

$$\rho(x) = a_0 + a_1(d/h - x/h)^{1/2} + b_1(x/h - s/(2h))^{1/2} \tag{25}$$

where $d = w + s/2$, when $s/2 < x < w + s/2$, and $\rho(x) = 0$ in other cases, the lower bound of the structure capacitance can be calculated. The coefficients a_0, a_1, and b_1 are variational parameters to be determined as in [4].

Assuming a constant gradient in the y-direction of ϵ_ξ^*, ϵ_η^*, or θ, the numerical studies have shown that a good convergence is achieved when $N = 20$. The normalized phase velocities of the quasi-static modes in a structure having constant $\epsilon_\xi^* = \epsilon_\eta^* = 2.55$, $\theta = 0$ at its ground plane, and a constant gradient of ϵ_η^* is plotted in Fig. 2. Changing ϵ_η^* by ϵ_ξ^*, Fig. 3 is obtained. Finally, in Fig. 4, a constant $\epsilon_\xi^* = 3.4$, $\epsilon_\eta^* = 5.12$, and a linear variation of the tilting angle from its value at the ground plane ($\theta = 0$) to its value at the interface ($\theta = \theta(h)$) have been assumed.

Despite their theoretical character at the moment, those studies can be a good starting point to further studies on the deformation or doping of a dielectric substrate, and other phenomena that imply a gradient of anisotropy. On the other hand, in Fig. 3, it is shown how high values of ϵ_ξ^* near the interface air–dielectric allow us to find equal values for the phase velocities of the even and odd modes, in agreement with [17].

V. Conclusions

With the help of the recurrence formulas (17) and (23), the transformed matrix Green's function (22) for any planar structure having arbitrary anisotropic substrates or superstrates can be easily constructed.

These simple recurrence formulas permit an easy computation by their direct insertion in the already existing programs. Furthermore, this method provides a suitable technique to calculate the characteristic parameters of structures having an arbitrary and smooth y-directed gradient of anisotropy.

Appendix

If the new variables

$$W_1^K = \beta F_1^K \Big/ \left(\prod_{n=1}^{K} \sinh(\beta h_n^{eq})\right) \tag{A1a}$$

$$W_2^K = \beta F_2^K \Big/ \left(\prod_{n=0}^{K-1} \sinh(\beta h_{N-n}^{eq})\right) \tag{A1b}$$

$$W_3^K = F_3^K \Big/ \left(\prod_{n=1}^{K} \sinh(\beta h_n^{eq})\right) \tag{A1c}$$

$$W_4^K = F_4^K \Big/ \left(\prod_{n=0}^{K-1} \sinh(\beta h_{N-n}^{eq})\right) \tag{A1d}$$

are defined, the following recurrence algorithm and final expressions can be obtained:

$$W_1^1 = -\frac{1}{\epsilon_1^{eq}} \tag{A2a}$$

$$W_2^1 = \frac{1}{\epsilon_N^{eq}} \tag{A2b}$$

$$W_3^1 = \coth(\beta h_1^{eq}) \tag{A2c}$$

$$W_4^1 = \coth(\beta h_N^{eq}) \tag{A2d}$$

$$W_1^{i+1} = \coth(\beta h_{i+1}^{eq}) W_1^i - \frac{1}{\epsilon_{i+1}^{eq}} W_3^i \tag{A2e}$$

$$W_2^{i+1} = \coth(\beta h_{N-i}^{eq}) W_2^i + \frac{1}{\epsilon_{N-i}^{eq}} W_4^i \tag{A2f}$$

$$W_3^{i+1} = \coth(\beta h_{i+1}^{eq}) W_3^i - \epsilon_{i+1}^{eq} W_1^i \tag{A2g}$$

$$W_4^{i+1} = \coth(\beta h_{N-i}^{eq}) W_4^i + \epsilon_{N-i}^{eq} W_2^i \tag{A2h}$$

$$G_{KL} = \frac{1}{\beta} \prod_{i=K+1}^{L} \left(\operatorname{csech}(\beta h_i^{eq})\right.$$
$$\left.\cdot \exp(j\beta R_i h_i)\right) \left\{ \frac{W_1^L W_4^{N-L}}{W_1^K W_2^{N-L}} - \frac{W_3^L}{W_1^K} \right\}^{-1} \tag{A3a}$$

$$G_{KK} = \frac{1}{\beta} \left\{ \frac{W_4^{N-K}}{W_2^{N-K}} - \frac{W_3^K}{W_1^K} \right\}^{-1}. \tag{A3b}$$

References

[1] R. P. Owens, J. E. Aitken, and T. C. Edwards, "Quasi-static characteristics of microstrip on an anisotropic sapphire substrate," *IEEE Trans. Microwave Theory Tech.*, vol. MTT-24, pp. 499–505, Aug. 1976.

[2] B. T. Szentkuti, "Simple analysis of anisotropic microstrip lines by a transform method," *Electron. Lett.*, vol. 12, pp. 672–673, Dec. 1976.

[3] M. Kobayashi and R. Terakado, "Accurately approximate formula for the effective filling fraction for microstrip lines with isotropic substrates and its application to the case with anisotropic substrate," *IEEE Trans. Microwave Theory Tech.*, vol. MTT-27, pp. 776–778, Sept. 1979.

[4] M. Horno, "Quasi-static characteristics of microstrip on arbitrary anisotropic substrates," *Proc. IEEE*, vol. 86, pp. 1033–1034, Aug. 1980.

[5] N. G. Alexopoulos, S. Kerner, and C. M. Krowne, "Dispersionless coupled microstrip over fused silica-like anisotropic substrate," *Electron. Lett.*, vol. 12, pp. 579–580, Oct. 1976.

[6] M. Kobayashi, "Analysis of the microstrip and the electrooptic light modulator," *IEEE Trans. Microwave Theory Tech.*, vol. MTT-26, pp. 119–126, Feb. 1978.

[7] M. Kobayashi and R. Terakado, "Method for equalizing phase velocities of coupled microstrip lines by using anisotropic substrates," *IEEE Trans. Microwave Theory Tech.*, vol. MTT-28, pp. 719–722, July 1980.

[8] M. Horno, "Upper and lower bounds on capacitances of coupled microstrip lines with anisotropic substrates," *Proc. Inst. Elec. Eng.*, vol. 129, pt. H, no. 3, pp. 89–93, June 1982.

[9] N. G. Alexopoulos and S. G. Maas, "Characteristics of microstrip directional couplers on anisotropic substrates," *IEEE Trans. Microwave Theory Tech.*, vol. MTT-30, pp. 1267–1270, Aug. 1982.

[10] M. Horno, "Quasistatic characteristics of covered coupled microstrip on anisotropic substrates: Spectral and variational analysis," *IEEE Trans. Microwave Theory Tech.*, vol. MTT-30, pp. 1888–1892, Nov. 1982.

[11] N. G. Alexopoulos and S. G. Maas, "Performance of microstrip couplers on an anisotropic substrate with an isotropic superstrate," *IEEE Trans. Microwave Theory Tech.*, vol. MTT-31, pp. 671–672, Aug. 1983.

[12] M. Horno, F. Medina, and R. Marqués, "Quasistatic characteristics of shielded coupled microstrip lines on anisotropic substrates," in *Proc. of II Int. IEEE Mediterranean Electrotech. Conf. (MELECON'83)*, (Athens, Greece), May 1983, pp. B5.05.

[13] S. K. Koul and B. Bath, "Generalized analysis of microstrip-like transmission lines and coplanar strips with anisotropic substrates for MIC, electrooptic modulator, and SAW applications," *IEEE Trans. Microwave Theory Tech.*, vol. MTT-31, pp. 1051–1059, Dec. 1983.

[14] T. Kitazawa and Y. Hayashi, "Coupled slot on an anisotropic sapphire substrate," *IEEE Trans. Microwave Theory Tech.*, vol. MTT-29, pp. 1035–1040, Oct. 1981.

[15] T. Kitazawa and Y. Hayashi, "Quasistatic characteristics of coplanar waveguides on a sapphire substrate with optical axes inclined," *IEEE Trans. Microwave Theory Tech.*, vol. MTT-30, pp. 920–922, June 1982.

[16] W. R. Smythe, *Static and Dynamic Electricity*. New York: McGraw Hill, 1968, ch. 3, pp. 54.

[17] M. Horno and R. Marqués, "Coupled microstrips on double anisotropic layers," *IEEE Trans. Microwave Theory Tech.*, vol. MTT-32, pp. 467–470, Apr. 1984.

Theoretical and Experimental Study of a Novel *H*-Guide Transverse Slot Antenna

M. KISLIUK, SENIOR MEMBER, IEEE, AND
A. AXELROD, STUDENT MEMBER, IEEE

***Abstract*—Transverse slots in the "upper" plate of a dielectric-loaded parallel plane waveguide (*H*-guide) operating in the dominant mode (zero cutoff frequency) are proposed as slot antennas.**

A new theoretical approach to the analysis of a single-slot antenna is presented, leading to explicit expressions for the antenna input impedance and radiation efficiency. The computed values of the VSWR and radiation efficiency are in good agreement with laboratory measurements. The radiation efficiency of a single slot exceeds 10 percent in the 8–11-GHz frequency band, reaching a 50-percent theoretically predicted maximum at the slot resonance frequency, when the guide is terminated by a matched load.

Experimental checks prove that the leakage, or parasitic, radiation power level is less than −40 dB relative to the measured radiated power.

Manuscript received July 20, 1984; revised January 4, 1985.

The authors are with the Department of Electron Devices and Electromagnetic Radiation, Faculty of Engineering, Tel-Aviv University, Tel-Aviv 69978, Israel.

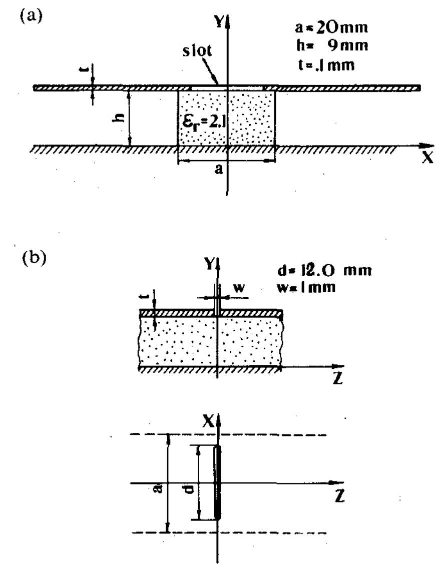

Fig. 1. (a) The *H*-guide cross section. (b) Geometry of the slot radiator.

I. Introduction

Microwave conformal antennas are widely used in many airborne and spaceborne systems. The conventionally used microstrip resonator antennas are mostly narrow band, have a poor radiation efficiency, and the parasitic radiation from the feeding microstriplines [1] interferes with the radiation from the resonator.

The *H*-guide proposed by F. J. Tisher [2], [3], or the parallel plane waveguide partially filled with a dielectric [4], can be fabricated as thin as a microstrip board, and successfully used for conformal mounting. M. Cohn showed [4] that "the dominant mode TE_{10}" of this guide (zero cutoff frequency) can be used for wide-band applications. The electric field of this mode is perpendicular to the metallic plates (Fig. 1), and neither the propagation constant, nor the wave impedance of this mode depend on the thickness of the guide. The fringe fields of the *H*-guide can be reduced to 60–80 dB by choosing the right width of the plates, thus excluding any leakage side radiation.

A theory of a single transverse, symmetrically spaced slot antenna (Fig. 1) is presented in Section II. Closed-form expressions for the normalized input impedance, the VSWR, and the radiation efficiency of a single-slot antenna are obtained. It is shown that 50 percent is the upper theoretical limit of the radiation efficiency of a single series slot radiator in any waveguide structure terminated by a matched load.

Laboratory measurements of the VSWR and radiation efficiency of a single slot (Figs. 5 and 6) are presented in Section III, and the measured values are in good agreement with the developed theory. The experiments confirm the theoretically predicted 50-percent radiation efficiency at VSWR = 3.0 of a single slot at resonance.

No significant change in the values of the reflected and transmitted waves has been detected when the measurements were repeated with metallic screens mounted across the side gaps of